Photoproduction of π^0 on Hydrogen with CLAS

Michael C. Kunkel,[1,*] Moskov J. Amaryan,[1,†] Igor I. Strakovsky,[2] James Ritman,[3,4] and Gary R. Goldstein[5]

[1] *Old Dominion University, Norfolk, VA 23529, USA*
[2] *The George Washington University, Washington, DC 20052, USA*
[3] *Institut für Kernphysik, Forschungszentrum Jülich, 52424 Jülich, Germany*
[4] *Institut für Experimentalphysik I, RuhrUniversität Bochum, 44780 Bochum, Germany*
[5] *Tufts University, Medford, MA 02155, USA*

Abstract

We report the first high precision measurement of exclusive π^0 photoproduction cross section in Dalitz decay and conversion mode on a hydrogen target in a wide kinematic range with the CLAS setup at Thomas Jefferson National Accelerator Facility. Measurement is performed in the reaction $\gamma p \to pe^+e^-X(\gamma)$ using a tagged photon beam spanning an energy interval from the "resonance" to the "Regge" regimes, i.e photon energies $E = 1.25 - 5.55$ GeV. The final state particles particles $p; e^+; e^-$ are detected while the photon is not detected. The π^0 is identified by analyzing the missing mass of proton. This new data quadrupled the world bremsstrahlung database above E = 2 GeV. Our data appear to favor the Regge pole model and the quark counting rule while disfavoring the Handbag model.

PACS numbers: 12.38.Aw, 13.60.Rj, 14.20.-c, 25.20.Lj

The rich $\pi + N$ resonance spectrum for center-of-mass (c.m.) energies up to 2.5 GeV provides insights and challenges concerning the workings of the strong interaction through partial wave expansions, exchange potentials, non-relativistic quark models and QCD. The π^0 and η photoproduction has always been a complementary tool to investigate and constrain the various models and lead to further insights. At the interface between the crowded low energy resonance cross section and the smooth higher energy behavior, traditionally described by Regge poles [1], lies a region in which hadronic duality provides an interpolation description of the cross section behavior. Exclusive π photoproduction and π nucleon elastic scattering show this duality in a semi-local sense through Finite Energy Sum Rules (FESR) [2]. The connection to QCD is more tenuous for on-shell photoproduction of pions at small scattering angles, but the quark content can become manifest through fixed angle dimensional counting rules [3] as well as being evident in semi-inclusive or exclusive electroproduction of pions, described through Transverse Momentum Distributions (TMDs) and Generalized Parton Distributions (GPDs).

This experiment is a unique opportunity to bridge resonance and high-energy, in particular, "Regge", regimes and increases the available database above the resonance range by a significant amount.

The Regge pole description of photoproduction amplitudes relies on already known Regge trajectories and coupling constants. The unitary cut amplitudes in meson photoproduction are interpreted as rescattering of on-shell meson-nucleon amplitudes. The phases between the poles and the elastic neutral pion re-scattering are critical in determining the polarizations and the constructive or destructive interferences that appear in the resonance spectrum.

The Regge pole and cut model for higher energies above the resonance regime for π^0 and η photoproduction developed by Goldstein and Owens [4] has the exchange of leading Regge trajectories with appropriate t-channel quantum numbers along with Regge cuts generated via final state rescattering through Pomeron exchange. There are two allowed t-channel J^{PC} quantum numbers series, the odd-signature 1^{--} and the 1^{+-}, corresponding to the ρ^0, ω, and the b_1^0, h_1 Reggeons, respectively. The Regge couplings to the nucleon were fixed by reference to electromagnetic form factors, $SU(3)_{flavor}$, and low energy nucleon-nucleon meson exchange potentials. The Primakoff effect is not included in the parameterization. Similar approaches to some extent were developed by Laget [5], Mathieu, Fox, and Szczepaniak [6], and recently, Donnachie and Kalashnikova [7]. The model of Laget is presumably valid within the full angular range ($\theta = 0^\circ - 180^\circ$) [5] while the others are good for different ranges of the forward direction, i.e. from $|t| = -t_{min}$ at $\theta = 0$ to $\theta = \pi/2$, where t is the squared four-momentum transfer. [4, 6, 7]. Here, we examine how Regge phenomenology works for the full CLAS energy range, i.e. E > 2.8 GeV.

The introduction of the handbag mechanism, developed by Kroll *et al.* [8], has provided complimentary possibilities for the interpretation of hard exclusive reactions. In this approach, the reaction is factorized into two parts, one quark from the incoming and one from the outgoing nucleon participate in the hard sub-process, which is calculable using pQCD. The soft part consists of all the other partons that are spectators and can be described in terms of GPDs [9]. The handbag model applicabil-

* Now at the Institut für Kernphysik, Forschungszentrum Jülich, 52424 Jülich, Germany
† Corresponding author; mamaryan@odu.edu

ity requires a hard scale, which, for meson photoproduction, is only provided by large transverse momentum. That corresponds to large angle production, roughly for $-0.6 \leq \cos\theta \leq 0.6$. Here, we examined how the handbag model may extend for the $\gamma p \to p\pi^0$ case as Kroll *et al.* proposed. Binary reactions in QCD, with large momentum transfer occur via gluon and quark exchanges between colliding particles. The quark counting rule of Brodsky and Farrar [3] has a simple recipe to predict the energy dependence of the differential cross sections of two-body reactions at large angles when t/s is finite and is kept constant. The lightest meson photoproduction was examined in terms of the counting rule [10–14]. As has been observed, first of all at SLAC by Anderson *et al.*, the reaction $\gamma p \to \pi^+ n$ shows agreement with constituent counting rules that predict the cross section should vary as s^{-7} [10]. The agreement extends down to s = 6 GeV^2 where baryon resonances are still playing a role. Here, we examined how the counting rule is applicable to the $\gamma p \to \pi^0 p$ up to s = 10 GeV^2.

Previous bremsstrahlung measurements for $2 \leq E \leq 18$ GeV (1964 – 1979) gave 451 data points $d\sigma/dt(|t|)$s for $\gamma p \to p\pi^0$ [15]. Existing bremsstrahlung world data on photoproduction of neutral pions on a proton target have very large systematic uncertainties and do not have sufficient accuracy to perform comprehensive phenomenological analyses. The recent tagged CLAS $g1c$ measurement has an overall systematic uncertainty of 5% and its contribution for $2 \leq E \leq 2.9$ GeV is limited to 164 $d\sigma/dt(|t|)$s [16].

In this work, we provide a large set of differential cross section values from E = 1.275–5.425 MeV in laboratory photon energy, corresponding to a range of c.m. energies, W, 1.81 – 3.33 GeV. We have compared the Regge pole, the handbag, and the quark counting rule phenomenology with the new CLAS experimental information on $d\sigma/dt(|t|)$ for the $\gamma p \to \pi^0 p$ reaction above the "resonance" regime. As will be seen, this data set quadruples the world bremsstrahlung database above E = 2 GeV and constrains the high energy phenomenology well with previous CLAS $g1c$ tagged measurements.

The experiment was performed with the CLAS setup at TJNAF using a tagged photon beam produced by bremsstrahlung from the 5.72 GeV electron beam provided by the CEBAF accelerator, which impinged upon a liquid hydrogen target. The experimental details are given in [17]. The reaction of interest is the photoproduction of neutral pions on a hydrogen target $\gamma p \to p\pi^0$, where the neutral pions were detected via external conversion, $\pi^0 \to \gamma\gamma \to e^+e^-\gamma$ and subsequent Dalitz decay $\pi^0 \to \gamma^*\gamma \to e^+e^-\gamma$. Running the experiment at high beam current was possible due to the final state containing three charged tracks, $p; e^+; e^-$, as opposed to single prong charged track detection, which impose limitations due to trigger and data acquisition restrictions.

Lepton identification was based on conservation of mass. Once the data was skimmed for p, π^+, π^-, all particles that were π^+, π^- were tentatively assigned to be electrons or positrons based on their charge (for details, see Ref. [20]). After particle selection, standard $g12$ calibration, fiducial cuts [17] and timing cuts were applied in the analysis.

The analysis employed three separate kinematic fitting hypotheses, 4-C, 1-C, and 2-C, as well as a cut on the missing energy of the detected system. The 4-C fit used the $\gamma p \to p\pi^+\pi^-$ channel to filter background from double charged pion production from single π^0 production. The 1-C fit was used for the topology of $\gamma p \to pe^+e^-(\gamma)$ to fit to a missing final state photon. The 2-C fit was used for the topology of $\gamma p \to pe^+e^-(\gamma)$ to fit to a missing final state photon but also to constrain the invariant mass of $e^+e^-(\gamma)$=m$^2_{\pi^0}$. The "confidence levels" for each constraint were consistent between g12 data and Monte-Carlo simulations.

The remainder of the background was attributed to $\pi^+\pi^-$ events. To reduce the background further, a comparison of the missing mass squared off the proton and the pe^+e^- missing energy of the system was performed, see Fig. 1. This comparison revealed that the majority of $\pi^+\pi^-$ background has missing energy less than 75 MeV. To eliminate this background all events with a missing energy less than 75 MeV were removed.

The distribution of the proton missing mass for events with $pe^+e^-(\gamma)$ in the final state is shown in Fig. 2. A fit is performed with the Crystal Ball function [18, 19] for the signal, plus a 3rd order polynomial function for the background. The total signal+background is shown by a red solid line. The fit results in $M^2_{\pi^0} = 0.0179$ GeV^2 and the Gaussian σ=0.0049 GeV^2. To select π^0 events, an asymmetric cut, from the measured mean value, was placed in the range $0.0056 \leq M^2_x(p) \leq 0.035$. This cut range can be seen as the red arrow in the bottom panel of Fig. 2 along with the ratio of background events to the total number of events. As shown in Fig. 2, the event selection strategy for this analysis allowed to have a negligible integrated background of no more than $\sim 1.05\%$.

Overall the systematic error is independent of the production angle and varies between 9% and 12% as a function of energy. The individual contributions came from particle efficiency, sector-to-sector efficiency, flux determination, missing energy cut, 4-C, 2-C, and 1-C probabilities, target length, branching ratio, fiducial cut, and the z-vertex cut.

The new CLAS high statistics cross sections, presented here, for $\gamma p \to \pi^0 p$ are compared in Figs. 3 and 4 with previous data from tagged JLab CLAS $g1c$ measurements [16], and bremsstrahlung DESY, Cambridge Electron Accelerator (CEA), and SLAC, and Electron Synchrotron at Cornell Univ. experiments [15]. The overall agreement is good, particularly with the tagged CLAS $g1c$ data.

At higher energies (above $s \sim 6$ GeV^2) and large c.m. angles ($\theta \geq 90^\circ$) in c.m., the results are consistent with the s^{-7} scaling, at fixed t/s, as expected from the quark counting rule [3]. The black dash-dotted line at 90° (Fig. 3) is a result of the fit of new CLAS $g12$ data only,

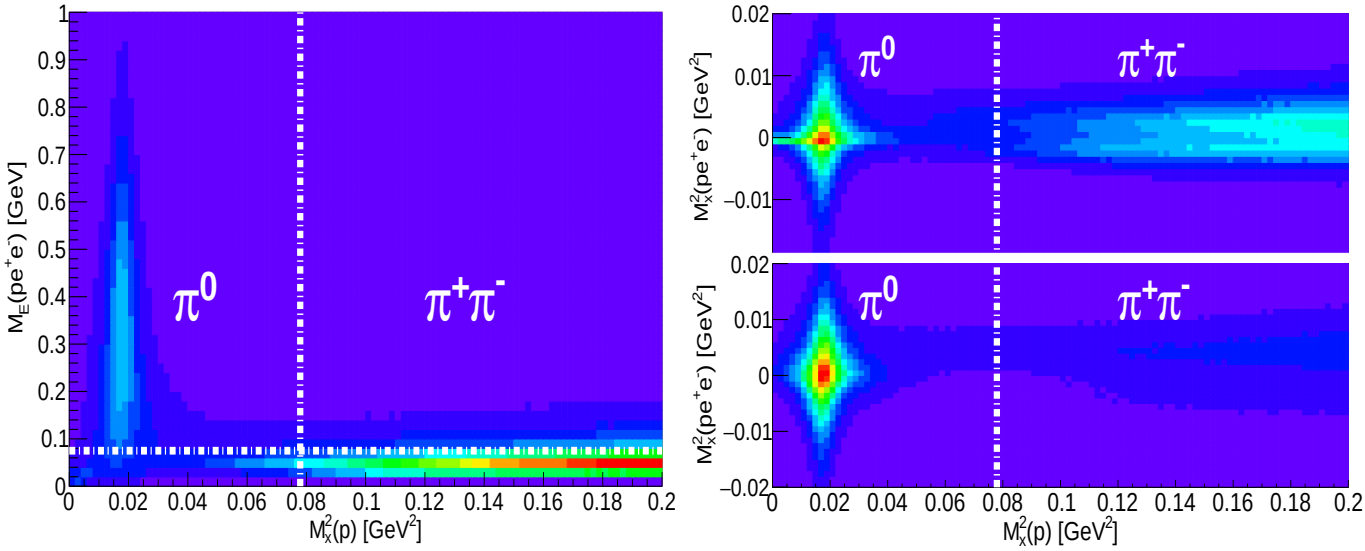

FIG. 1: (Color online)(left panel)M_x^2(p) vs. $M_E(pe^+e^-)$. (Right panel)M_x^2(p) vs. $M_x^2(pe^+e^-)$;(right-top panel)before applying the $M_E(pe^+e^-) < 75$ MeV condition, (right-bottom panel) after applying the $M_E(pe^+e^-) < 75$ MeV condition. The horizontal white dashed-dotted line depicted on the left panel illustrates the 75 MeV threshold used in this analysis. The vertical white dashed-dotted line depicts the kinematic threshold for $\pi^+\pi^-$ production.

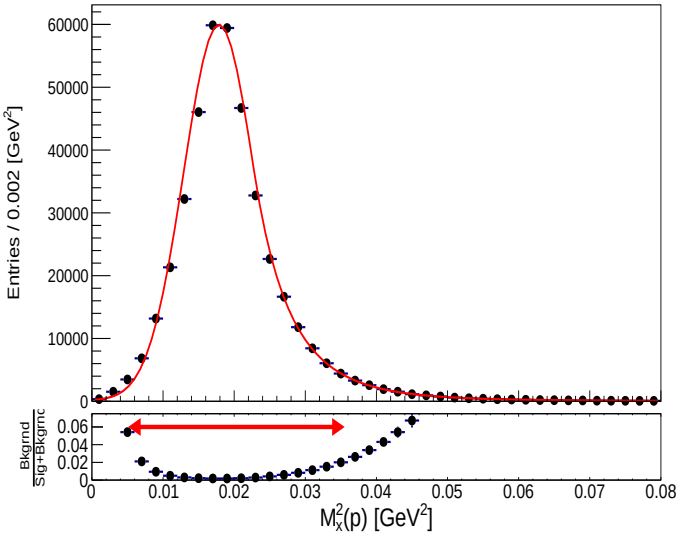

FIG. 2: (Color online) (top-panel)Peak of π^0 in the missing mass of proton for events with $pe^+e^-(\gamma)$ in the final state. The red-solid line depicts the fit function (signal+background). (bottom-panel) Relative contributions of $\frac{\text{Background}}{\text{Signal+Background}}$. The red arrow indicates the cut placed on the $M_x^2(p)$ distribution to select π^0 events.

performed with a power function $\sim s^{-n}$, leading to n = 6.89±0.26. Oscillations observed at 50° and 70° up to s∼10 GeV^2 indicate that the quark counting rule requires higher energies and higher $|t|$ before it can provide a valid description.

In Figs. 4 and 5, the $d\sigma/dt(|t|)$ values are shown along with predictions from Regge pole and cut [4–7] models and the handbag [8] model.

Below $|t|$ ∼0.6 GeV^2 there is a small difference between different Regge approaches. Overall, the Regge approximation becomes less relevant below E = 3 GeV (Fig. 4). This CLAS data make this statement more apparent. Note that some small structures start to appear around $|t| = 0.3-0.6$ GeV^2 ($\cos\theta = 0.6-0.8$) below E = 4 GeV. The dip around $|t| = 0.9-1.2$ GeV^2 ($\cos\theta = 0.2-0.4$) (moving with energy) agrees with the presented CLAS data. This is surprising since there was no previous indication of this dip. Note that the Regge amplitudes imposes non negligible constraints for the "resonance" region. Our data show two more visible dips above E = 4 GeV and around $|t|$ ∼3 GeV^2 and $|t|$ ∼5 GeV^2. The Regge model predicts nonsense, wrong signature zeroes, where the Regge trajectories cross negative even integers. For the dominant vector meson Regge poles, these dips should appear at approximately $-t = 0.6$, 3.0, 5.0 GeV^2, which agrees with the data. That is why it is also important to study the high energy region, above "resonance" regime.

The Reggeon trajectories and cancellation of singularities in $|t|$ gives rise to zeroes in the various combinations of helicity amplitudes. These are seen as dips in the cross sections. Dips that occur for one Regge trajectory are filled in by the contributions from other, distinct trajectories. That is, the zeroes for the ρ^0, ω trajectories occur at different values of $|t|$ than those of the b_1^0, h_1 trajectories. Nevertheless, because the two sets have opposite naturality (parity $(-1)^J$ or $(-1)^{J+1}$), there are combinations of helicity amplitudes that will separate into "natural" and "unnatural" parity. Those would have zeroes separately. Since zeroes are not observed, but dips are, a mechanism for producing those dips is provided by final

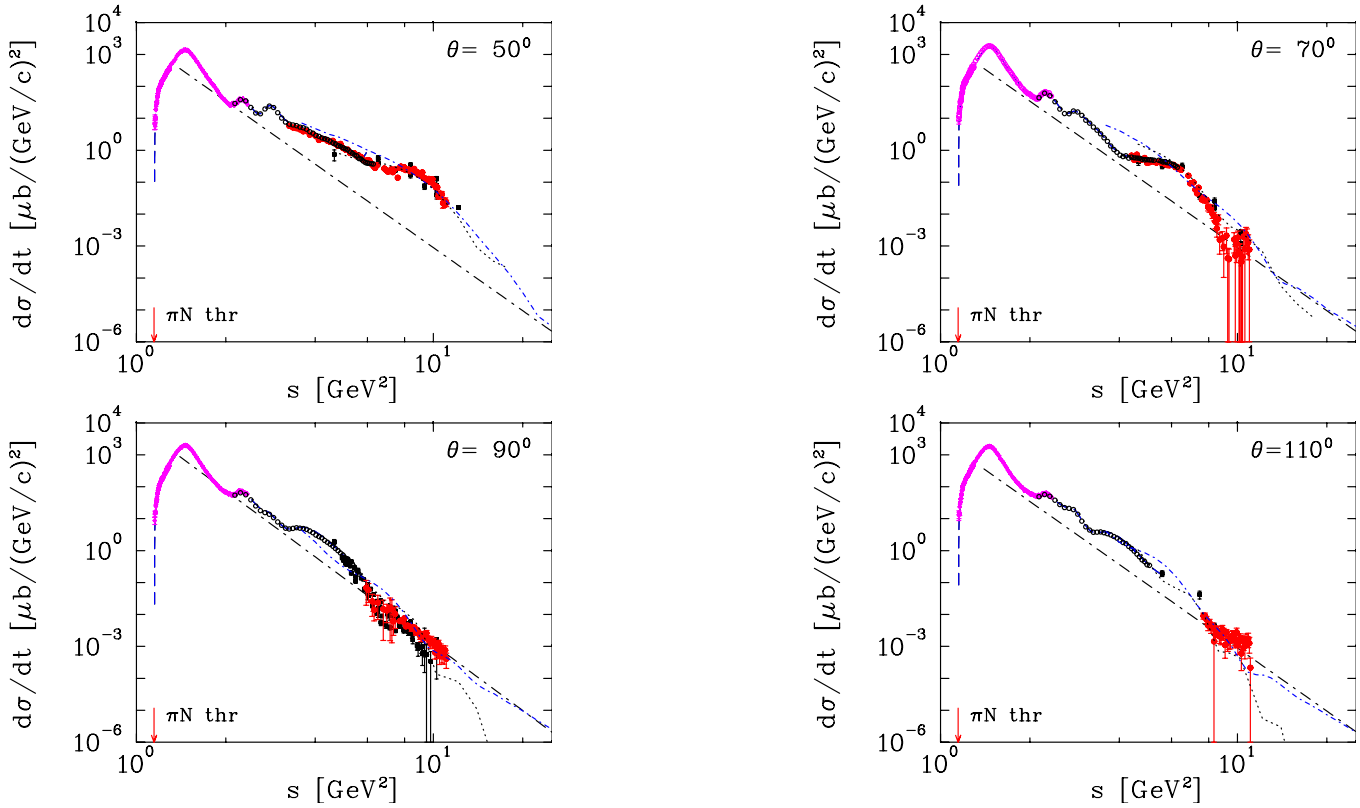

FIG. 3: (Color online) Differential cross section of $\gamma p \to \pi^0 p$ dσ/dt(s) at polar angles of 50°, 70°, 90°, and 110° in the c.m. frame as a function of c.m. energy squared, s. The red filled circles are the current $g12$ data. The recent tagged data are from CLAS $g1c$ [16] (black open circles) and the A2 at MAMI Collaboration [21] (magenta open diamonds with crosses). While black open filled squares are data from old bremsstrahlung measurements above E = 2 GeV [15]. Plotted uncertainties are statistical. The blue dashed line corresponds to the SAID PWA DU13 solution (no new CLAS data are used for the fit) [22]. Black dot-dashed lines are plotted as the best fit result for the spectrum at 90°. Pion production threshold shown as a vertical red arrow. Regge results [4, 5] are given by black dotted and blue dash-dotted, respectively.

state interactions which correspond to Regge cuts (for an alternative Regge cut model see, for instance, Ref. [5]). Those were implemented in an eikonal formalism. It was expected that the appropriate range of $|t|$ was roughly $0 < |t| < 1.3$ GeV^2. Since these data cover that full range of $|t|$, it is interesting to see how the old model, for instance [4], fares in an enlarged range. Remarkably, with a lowering of the original Pomeron strength, the model agrees with the data fairly well up to the 90°. The description of the π^0 photoproduction cross sections at largest $|t|$ requires some improvement of the Regge model probably by including u-channel exchange.

Simultaneously, Fig. 5 shows that the new CLAS data are orders of magnitude higher than the handbag model for π^0 photoproduction below $s = 11$ GeV^2 (solid blue line).

A significant increase in the comprehensiveness of the database for observables in the meson photoproduction process is critical to reaching definitive knowledge about QCD-based models of the nucleon. Studies that cover a broad range of c.m. energy $\sqrt{s}$ are particularly helpful in sorting out the phenomenology.

Through the experiments described above, an extensive and precise data set (2030 data points) on the differential cross section for π^0 photoproduction from the proton has been obtained over the range of $1.81 \leq W \leq 3.33$ GeV. A novel approach based on the use of the Dalitz decay mode was employed for extracting the cross sections from the experimental data. Measurements are performed in the reaction $\gamma p \to p e^+ e^- X(\gamma)$ using a tagged photon beam spanning the energy interval covered by "resonance" and "Regge" regimes.

The measurements obtained here have been compared to existing data. The overall agreement is good, while the data provided here quadrupled the world bremsstrahlung database above E = 2 GeV and covered the previous reported energies with finer resolution. By comparing this new and greatly expanded data set to the predictions of several phenomenological models, the present data were found to favor the Regge pole model and quark counting rule while disfavoring the handbag approach.

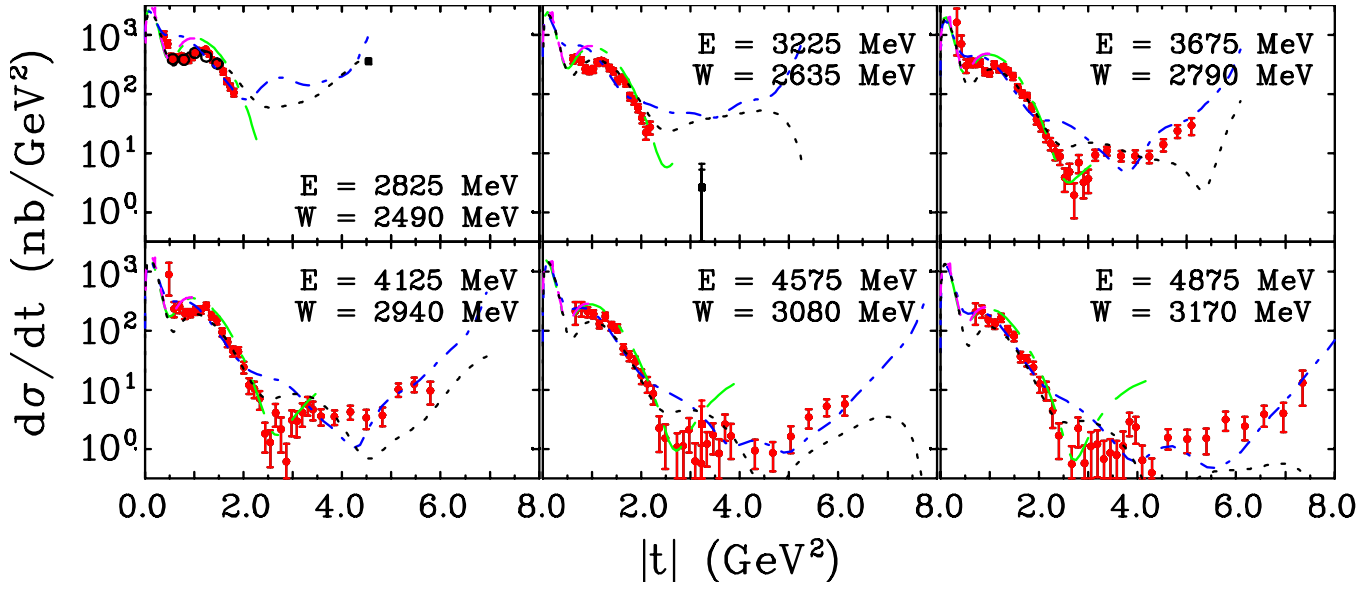

FIG. 4: (Color online) Samples of the π^0 photoproduction cross section, $d\sigma/dt(|t|)$, off the proton versus $|t|$ above "resonance" regime. Tagged experimental data are from the current CLAS $g12$ (red filled circles) and CLAS $g1c$ [16] (black open circles). The plotted points from previously published bremsstrahlung experimental data above E = 2 GeV [15] (black filled squares) are those data points within $\Delta E = \pm 3$ MeV of the photon energy in the laboratory system indicated on each panel. The uncertainties plotted are only the statistical errors. Regge results [4–7] are given by black dotted, blue short dash-dotted, green long dash-dotted, and magenta long dashed lines, respectively.

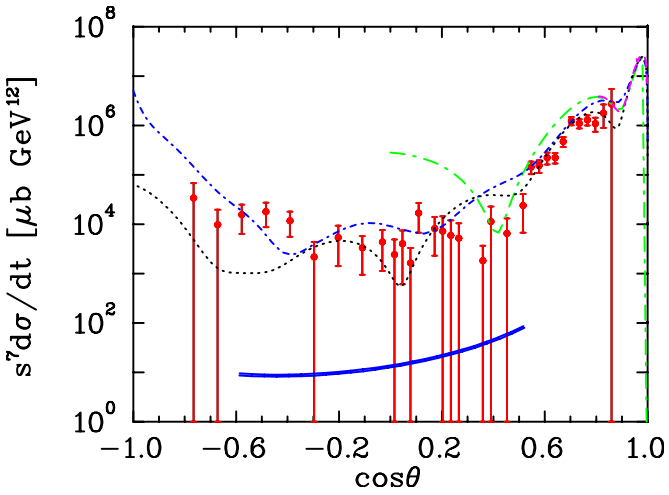

FIG. 5: (Color online) Differential cross section of π^0 photoproduction. The CLAS experimental data at s = 11 GeV^2 are from the current $g12$ experiment (red filled circles). The theoretical curves for the Regge fits are the same as in Fig. 4 and the handbag model by Kroll *et al.* [8] at $s = 10$ GeV^2 (blue double solid line).

We thank Stanley Brodsky, Alexander Donnachie, Peter Kroll, Jean-Marc Laget, Vincent Mathieu, and Anatoly Radyushkin for discussions of our measurements. We would like to acknowledge the outstanding efforts of the staff of the Accelerator and the Physics Divisions at Jefferson Lab that made the experiment possible. This work was supported in part by the Italian Istituto Nazionale di Fisica Nucleare, the French Centre National de la Recherche Scientifique and Commissariat à l'Energie Atomique, the United Kingdom's Science and Technology Facilities Council (STFC), the U.S. DOE and NSF, and the Korea Science and Engineering Foundation. The Southeastern Universities Research Association (SURA) operates the Thomas Jefferson National Accelerator Facility for the US DOE under contract DEAC05–84ER40150.

[1] J. P. Ader, M. Capdeville, and Ph. Salin, Nucl. Phys. **B3**, 407 (1967).
[2] H. K. Armenian, G. R. Goldstein, J. P. Rutherfoord, and D. L. Weaver, Phys. Rev. D **12**, 1278 (1975).
[3] S. J. Brodsky and G. R. Farrar, Phys. Rev. Lett. **31**, 1153 (1973).
[4] G. R. Goldstein and J. F. Owens III, Phys. Rev. D **7**, 865 (1973).
[5] J.-M. Laget, Phys. Rev. C **72**, 022202(R) (2005).
[6] V. Mathieu, G. Fox, and A. Szczepaniak, Phys. Rev. D

92, 074013 (2015).
[7] A. Donnachie and Yu. S. Kalashnikova, Phys. Rev. C **93**, 025203 (2016).
[8] H. W. Huang and P. Kroll, Eur. Phys. J. C **17**, 423 (2000); H. W. Huang, R. Jakob, P. Kroll, and K. Passek-Kumericki, Eur. Phys. J. C **33**, 91 (2004); M. Diehl and P. Kroll, arXiv:1302.4604 [hep–ph].
[9] X. Ji, Phys. Rev. Lett. **78**, 610 (1997); Phys. Rev. D **55**, 7114 (1997); A. V. Radyushkin, Phys. Lett. B **380**, 417 (1996); Phys. Rev. D **56**, 5524 (1997); D. Muller, *et al.*
[10] R. L. Anderson *et al.*, Phys. Rev. D **14**, 679 (1976).
[11] D. A. Jenkins and I. I. Strakovsky, Phys. Rev. C **52**, 3499 (1995).
[12] L. Y. Zhu *et al.* (Jefferson Lab Hall A Collaboration), Phys. Rev. Lett. **91**, 022003 (2003).
[13] W. Chen *et al.* (CLAS Collaboration), Phys. Rev. Lett. **103**, 012301 (2009).
[14] Kook-Jin Kong, Tae Keun Choi, and Byung-Geel Yu, Phys. Rev. C **94**, 025202 (2016).
[15] The Durham HEP Reaction Data Databases (UK) (Durham HepData): http://durpdg.dur.ac.uk/hepdata/reac.html .
[16] M. Dugger *et al.* (CLAS Collaboration), Phys. Rev. C **76**, 025211 (2007).
[17] G12 experimental group, CLAS-NOTE 2017 - 002, 2017 `https://misportal.jlab.org/ul/Physics/Hall-B/clas/viewFile.cfm/2017-002.pdf?documentId=756`.
[18] M. J. Oreglia, SLAC-236 UC-34d (T/E/I). Ph. D. Dissertation, SLAC, 1980.
[19] T. Skwarnicki, DESY F31-86-02, Ph. D. Dissertation, Inst. of Nucl. Phys. Cracow, Poland, 1986.
[20] M. C. Kunkel, Ph. D. Dissertation, Old Dominion University, 2014. `https://drive.google.com/open?id=0B9hZ1JQSJmToWnlNRFVycjRnUVE`
[21] M. Fuchs *et al.*, Phys. Lett. B **368**, 20 (1996); R. Beck *et al.*, Eur. Phys. J. A **28S1**, 173 (2006).
[22] M. Dugger *et al.* (CLAS Collaboration), Phys. Rev. C **88**, 065203 (2013).